

A MICROSCOPIC $NN \rightarrow NN^*(1440)$ POTENTIAL

B. Juliá-Díaz^{1,2}, A. Valcarce², P. González³ and F. Fernández²

¹ Department of Physical Sciences, University of Helsinki and Helsinki Institute of Physics, P.O. Box 64, 00014 Helsinki, Finland

² Grupo de Física Nuclear, Universidad de Salamanca, E-37008 Salamanca, Spain

³ Dpto. de Física Teórica and IFIC, Universidad de Valencia - CSIC, E-46100 Burjassot, Valencia, Spain

Received: date / Revised version: date

Abstract. By means of a $NN \rightarrow NN^*(1440)$ transition potential derived in a parameter-free way from a quark-model based NN potential, we determine simultaneously the $\pi NN^*(1440)$ and $\sigma NN^*(1440)$ coupling constants. We also present a study of the target Roper excitation diagram contributing to the $p(d, d')$ reaction.

PACS. 12.39.Jh Nonrelativistic quark model – 13.75.Cs Nucleon-nucleon interactions

1 Introduction

The $N^*(1440)$ (Roper) is a broad resonance which couples strongly (60–70%) to the πN channel and significantly (5–10%) to the σN channel [1]. These features suggest that the Roper resonance should play an important role in nuclear dynamics as an intermediate state. Graphs involving the excitation of $N^*(1440)$ appear in different systems, as for example the three-nucleon interaction mediated by π and σ exchange contributing to the triton binding energy [2]. The excitation of the Roper resonance has also been used to explain the missing energy spectra in the $p(\alpha, \alpha')$ reaction [3] or the $np \rightarrow d(\pi\pi)^0$ reaction [4]. The coupling of the $N^*(1440)$ to πN and σN channels could also be important in heavy ion collisions at relativistic energies [5, 6]. Finally, pion electro- and photoproduction may take place through the $N^*(1440)$ excitation [7]. However the use of a $NN \rightarrow NN^*(1440)$ transition potential as a straightforward generalization of some pieces of the $NN \rightarrow NN$ potential plus the incorporation of resonance width effects may have serious shortcomings specially concerning the short-range part of the interaction [8].

In this talk we present some applications of a recently derived $NN \rightarrow NN^*(1440)$ interaction [9], obtained by means of the same quark-model approach previously used to study the NN system and transition potentials involving the Δ . A main feature of the quark treatment is its universality in the sense that all the baryon-baryon interactions are treated on an equal footing. Moreover, once the model parameters are fixed from NN data there are no free parameters for any other case. This allows a microscopic understanding and connection of the different baryon-baryon interactions that is beyond the scope of any analysis based only on effective hadronic degrees of freedom. These studies are instructive inasmuch as they are expected to lead to a deeper understanding of the nu-

clear potential and entail a rethinking of basic nuclear concepts from the point of view of the fundamental quark substructure. We center our attention in the derivation of the $\pi NN^*(1440)$ and $\sigma NN^*(1440)$ coupling constants and in the study of a reaction mediated by the excitation of the Roper resonance, the $p(d, d')$ reaction.

2 $\pi NN^*(1440)$ and $\sigma NN^*(1440)$ coupling constants.

The usual way to determine meson- NN coupling constants is through the fitting of NN scattering data with phenomenological meson exchange models. Therefore, a consistent way to obtain meson- NN^* coupling constants is from a transition $NN \rightarrow NN^*$ potential, in particular when ratios over meson- NN coupling constants are to be considered. In order to derive the transition potential we shall follow the same quark model approach previously used for NN scattering [10]. Explicitly, the $NN \rightarrow NN^*(1440)$ potential at interbaryon distance R is obtained by sandwiching the qq potential, V_{qq} , between NN and $NN^*(1440)$ states, written in terms of quarks, for all the pairs formed by two quarks belonging to different baryons. The qq potential contains a confining term taken to be linear (r_{ij}), the usual perturbative one-gluon-exchange (OGE) interaction containing Coulomb ($1/r_{ij}$), spin-spin ($\sigma_i \cdot \sigma_j$) and tensor (S_{ij}) terms, and pion and sigma exchanges as a consequence of the breaking of chiral symmetry. The wave function of the Roper, $N^*(1440)$, and nucleon, N , states can be written as $|N^*(1440)\rangle = \left\{ \sqrt{\frac{2}{3}}|[3](0s)^2(1s)\rangle - \sqrt{\frac{1}{3}}|[3](0s)(0p)^2\right\} \otimes [1^3]_c$ and $|N\rangle = |[3](0s)^3\rangle \otimes [1^3]_c$ where $[1^3]_c$ is the completely antisymmetric color state, $[3]$ is the completely symmetric spin-isospin

state and $0s$, $1s$, and $0p$, stand for harmonic oscillator orbitals.

The transition potential obtained can be written at all distances in terms of baryonic degrees of freedom [11]. One should realize that a qq spin and isospin independent potential as for instance the scalar one-sigma exchange (OSE), gives rise at the baryon level, apart from a spin-isospin independent potential, to a spin-spin, an isospin-isospin and a spin-isospin dependent interactions [9]. Nonetheless for distances $R \geq 4$ fm, where quark antisymmetrization interbaryon effects vanish, we are only left with the direct part, i.e. with a scalar OSE at the baryon level. The same kind of arguments can be applied to the one-pion exchange (OPE) potential. Thus asymptotically ($R \geq 4$ fm) OSE and OPE have at the baryon level the same spin-isospin structure than at the quark level. Hence we can parametrize the asymptotic central interactions as

$$V_{NN \rightarrow NN^*(1440)}^{OPE}(R) = \frac{1}{3} \frac{g_{\pi NN}}{\sqrt{4\pi}} \frac{g_{\pi NN^*(1440)}}{\sqrt{4\pi}} \frac{m_\pi}{2M_N} \frac{m_\pi}{2(2M_\tau)} \frac{\Lambda^2}{\Lambda^2 - m_\pi^2} [(\boldsymbol{\sigma}_N \cdot \boldsymbol{\sigma}_N)(\boldsymbol{\tau}_N \cdot \boldsymbol{\tau}_N)] \frac{e^{-m_\pi R}}{R}, \quad (1)$$

and

$$V_{NN \rightarrow NN^*(1440)}^{OSE}(R) = - \frac{g_{\sigma NN}}{\sqrt{4\pi}} \frac{g_{\sigma NN^*(1440)}}{\sqrt{4\pi}} \frac{\Lambda^2}{\Lambda^2 - m_\sigma^2} \frac{e^{-m_\sigma R}}{R}, \quad (2)$$

where g_i stands for the coupling constants at the baryon level and M_τ is the $NN^*(1440)$ reduced mass.

By comparing the baryonic potentials with the asymptotic behavior of the ones previously obtained from the quark-model calculation we can extract the $\pi NN^*(1440)$ and $\sigma NN^*(1440)$ coupling constants. As the parameters at the quark level are fixed once for all from the NN interaction our results allow a prediction of these constants in terms of the elementary πqq coupling constant and the one-baryon model dependent structure. The sign obtained for the meson- $NN^*(1440)$ coupling constants and for their ratios to the meson- NN coupling constants is ambiguous since it comes determined by the arbitrarily chosen relative sign between the N and $N^*(1440)$ wave functions. Only the ratios between the $\pi NN^*(1440)$ and $\sigma NN^*(1440)$ would be free of this uncertainty. This is why we will quote absolute values except for these cases where the sign is a clear prediction of the model. To get such a prediction we can use any partial wave. We shall use for simplicity the 1S_0 wave, this is why we only wrote the central interaction in Eq. (1).

The $[\Lambda^2/(\Lambda^2 - m_i^2)]$ factor comes from the vertex form factor chosen at momentum space as a square root of monopole $[\Lambda^2/(\Lambda^2 + \mathbf{q}^2)]^{1/2}$, the same choice taken at the quark level, where chiral symmetry requires the same form for pion and sigma. A different choice for the form factor at the baryon level, regarding its functional form as well as the value of Λ , would give rise to a different vertex factor and eventually to a different functional form

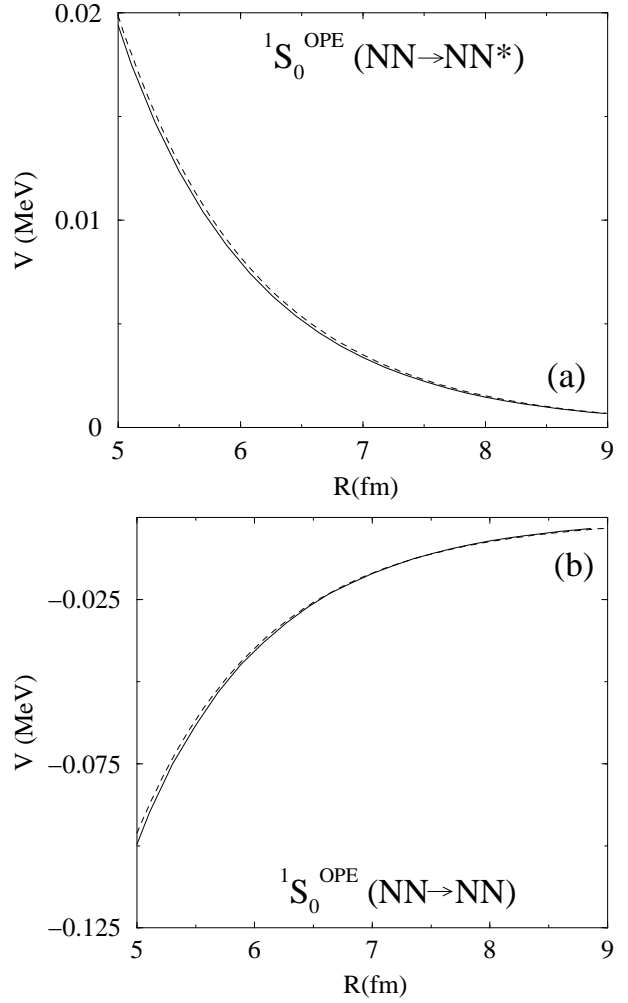


Fig. 1. (a) Asymptotic behavior of the one-pion exchange 1S_0 $NN \rightarrow NN^*(1440)$ potential (solid line). The dashed line denotes the fitted curve according to Eq. (1). (b) Same as (a) but for the one-pion exchange 1S_0 $NN \rightarrow NN$ potential.

for the asymptotic behavior. For instance, for a modified monopole form, $[(\Lambda^2 - m^2)/(\Lambda^2 - \mathbf{q}^2)]^{1/2}$, where m is the meson mass (m_π or m_σ), the vertex factor would be 1, i.e. $[(\Lambda^2 - m^2)/(\Lambda^2 - m^2)]$, keeping the potential the same exponentially decreasing asymptotic form. Then it is clear that the extraction from any model of the meson-baryon-baryon coupling constants depends on this choice. We shall say they depend on the coupling scheme.

For the one-pion exchange and for our value of $\Lambda = 4.2$ fm $^{-1}$, $[\Lambda^2/(\Lambda^2 - m_\pi^2)] = 1.03$, pretty close to 1. As a consequence, in this case the use of our form factor or the modified monopole form at baryonic level makes little difference in the determination of the coupling constant. This fact is used when fixing $g_{\pi qq}^2/4\pi$ from the experimental value of $g_{\pi NN}^2/4\pi$ extracted from NN data.

To get $g_{\pi NN^*(1440)}/\sqrt{4\pi}$ we turn to our results for the 1S_0 OPE potential, Fig. 1, and fit its asymptotic behavior

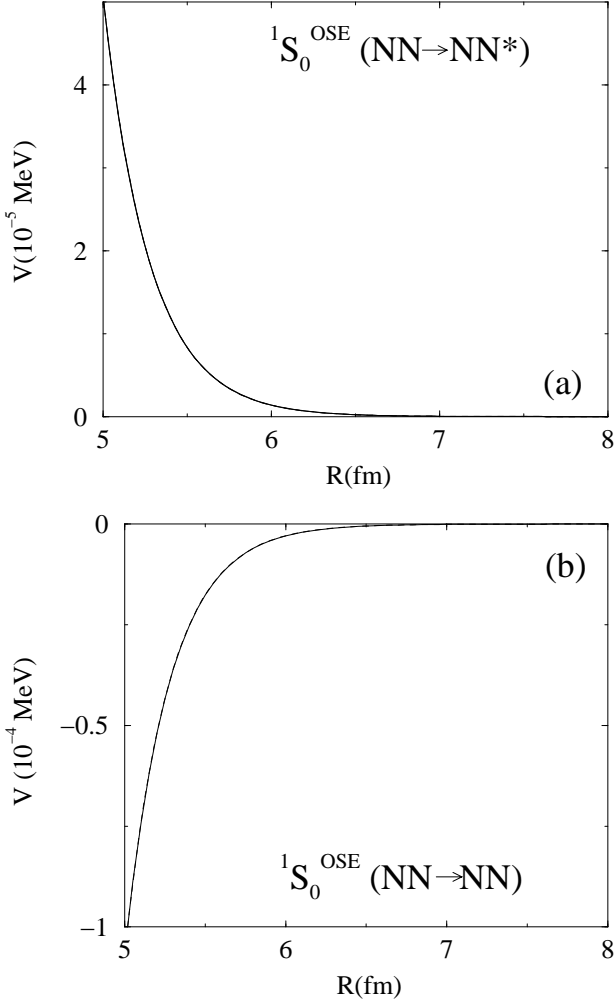


Fig. 2. (a) Asymptotic behavior of the one-sigma exchange 1S_0 $NN \rightarrow NN^*(1440)$ potential (solid line). The dashed line denotes the fitted curve according to Eq. (2). (b) Same as (a) but for the one-sigma exchange 1S_0 $NN \rightarrow NN$ potential.

(in the range $R : 5 \rightarrow 9$ fm) to Eq. (1). We obtain

$$\frac{g_{\pi NN}}{\sqrt{4\pi}} \frac{g_{\pi NN^*(1440)}}{\sqrt{4\pi}} \frac{\Lambda^2}{\Lambda^2 - m_\pi^2} = -3.73, \quad (3)$$

i.e. $g_{\pi NN^*(1440)}/\sqrt{4\pi} = -0.94$. As explained above only the absolute value of this coupling constant is well defined. Let us note that in Ref. [12] a different sign with respect to our coupling constant is obtained what is a direct consequence of the different global sign chosen for the $N^*(1440)$ wave function. The coupling scheme dependence can be explicitly eliminated if we compare $g_{\pi NN^*(1440)}$ with $g_{\pi NN}$ extracted from the $NN \rightarrow NN$ potential within the same quark model approximation, Fig. 1. Thus we get

$$\left| \frac{g_{\pi NN^*(1440)}}{g_{\pi NN}} \right| = 0.25. \quad (4)$$

By proceeding in the same way for the OSE potential, i.e. by fitting the potential given in Fig. 2(a) to Eq. (2),

and following an analogous procedure for the NN case, Fig. 2(b), we can write

$$\left| \frac{g_{\sigma NN^*(1440)}}{g_{\sigma NN}} \right| = 0.47. \quad (5)$$

The ratio given in Eq. (4) is similar to that obtained in Ref. [12] and a factor 1.5 smaller than the one obtained from the analysis of the partial decay width. Nonetheless one can find in the literature values for $f_{\pi NN^*(1440)}$ ranging between 0.27–0.47 coming from different experimental analyses with uncertainties associated to the fitting of parameters [4, 6, 7].

Regarding the ratio obtained in Eq. (5), our result agrees quite well with the only experimental available result, obtained in Ref. [13] from the fit of the cross section of the isoscalar Roper excitation in $p(\alpha, \alpha')$ in the 10–15 GeV region, where a value of 0.48 is given. Furthermore, we can give a very definitive prediction of the magnitude and sign of the ratio of the two ratios,

$$\frac{g_{\pi NN^*(1440)}}{g_{\pi NN}} = 0.53 \frac{g_{\sigma NN^*(1440)}}{g_{\sigma NN}}, \quad (6)$$

which is an exportable prediction of our model.

3 Roper excitation in pd scattering

There are two experiments where the contribution from the $N^*(1440)$ resonance has been isolated by means of model-dependent theoretical methods. The first one is the $p(\alpha, \alpha')$ reaction carried out in Saclay [14] already ten years ago. The data showed two peaks in the cross section that were not understood for some years. The most prominent one was attributed to a Δ excitation in the projectile (DEP) [15]. The second peak was explained when a Roper excitation in the target (RET) was considered [3] giving a plausible explanation to the measured differential cross section.

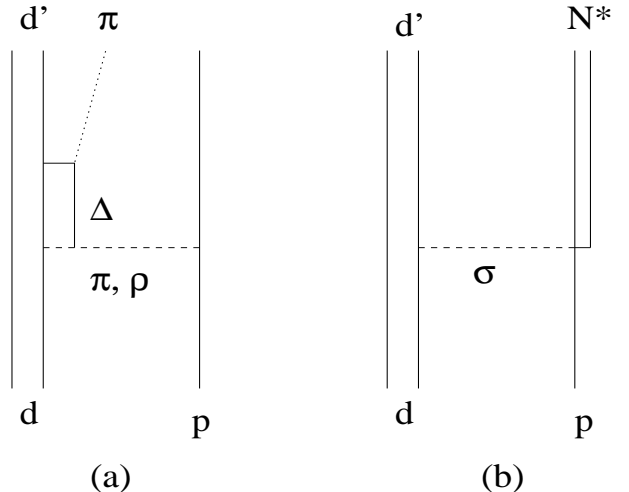


Fig. 3. Dominant mechanisms contributing to the $p(d, d')$ reaction [16].

The second experiment is the $p(d, d')$ reaction. It was considered and studied making use of the same mechanisms [16]. In Fig. 3 we show the two diagrams which give the bulk contribution to the cross section of the processes.

These two reactions are particularly interesting because in both cases the projectile (d or α) has $T = 0$. This ensures that the $N^*(1440)$ reaction mechanism, Fig. 3(b), can only be driven by a scalar interaction. Therefore these reactions have provided a method to determine the baryonic coupling constant between the N , $N^*(1440)$ and the σ meson once the Δ contribution has been fixed. The results for the coupling constants obtained in this way from $p(\alpha, \alpha')$ have been quoted and compared to ours in the previous section. Our purpose in this section is the study of the $p(d, d')$ process making use of the quark model $NN \rightarrow NN^*(1440)$ transition potential, to explore the mechanism proposed in Ref. [16]. The differential cross section for the process is given by:

$$\frac{d^2\sigma}{dE_{d'}d\Omega_{d'}^L} = \frac{p_{d'}}{(2\pi)^5} \frac{M_d^2 M^2}{\lambda^{1/2}(s, M^2, M_d^2)} \times \int \frac{d^3p_\pi}{E_{N'}\omega_\pi} \bar{\Sigma}\Sigma|T|^2 \delta(E_d + E_N - E_{d'} - E_{N'} - \omega_\pi), \quad (7)$$

where $M(M_d)$ is the nucleon (deuteron) mass, s is the invariant mass of the $p-d$ system, $\lambda(x, y, z) = x^2 + y^2 + z^2 - 2xy - 2yz - 2xz$ and $\bar{\Sigma}\Sigma|T|^2$ is the amplitude for the elementary process of $N^*(1440)$ production. This amplitude can be written in terms of the scalar transition potential $(V_0)_{NN \rightarrow NN^*}$ [16]:

$$\bar{\Sigma}\Sigma|T|^2 = 12F_d^2 \left(\frac{f'}{m_\pi} \right)^2 |G^*|^2 |(V_0)_{NN \rightarrow NN^*}(q_{cm})|^2 q_{cm}^2. \quad (8)$$

The function $F_d(\mathbf{k})$ is the deuteron form factor defined as

$$F_d(\mathbf{k}) = \int d\mathbf{r} \phi^*(\mathbf{r}) e^{i\frac{\mathbf{k}\cdot\mathbf{r}}{2}} \phi(\mathbf{r}) \quad (9)$$

where $\phi(\mathbf{r})$ is the deuteron S-wave function, and the momentum $\mathbf{k} = \mathbf{p}_d - \mathbf{p}_{d'}$ is taken in the initial deuteron rest frame. q_{cm} is the momentum transfer between the nucleons in the center of mass system and $f' \equiv f_{\pi NN^*}$. G^* is the $N^*(1440)$ propagator as given in Ref. [16].

We evaluate the cross section in the center of mass system and then relate the result to the one which is shown by the experimentalists making use of:

$$\frac{d^2\sigma}{dE_{d'}d\Omega_{d'}^L} = \frac{d^2\sigma}{dE_{d'}d\Omega_{d'}^{cm}} \frac{d\Omega_{d'}^{cm}}{d\Omega_{d'}^L}. \quad (10)$$

For the kinematics considered it can be shown that

$$\frac{d\Omega_{d'}^{cm}}{d\Omega_{d'}^L} = \frac{p_d^L p_{d'}^L}{p_d^{cm} p_{d'}^{cm}} \left(1 - \frac{E_d^{cm}}{\sqrt{s}} \right) + \frac{\cos(\theta^{cm})}{p_{d'}^{cm} 2} \frac{E_{d'}^{cm}}{\sqrt{s}} p_d^L p_{d'}^L. \quad (11)$$

In order to perform the calculation using our quark model, we need to extract the genuine scalar potential at all distances from our $NN \rightarrow NN^*(1440)$ transition potential. At short distances, $R < 2$ fm, the quark model

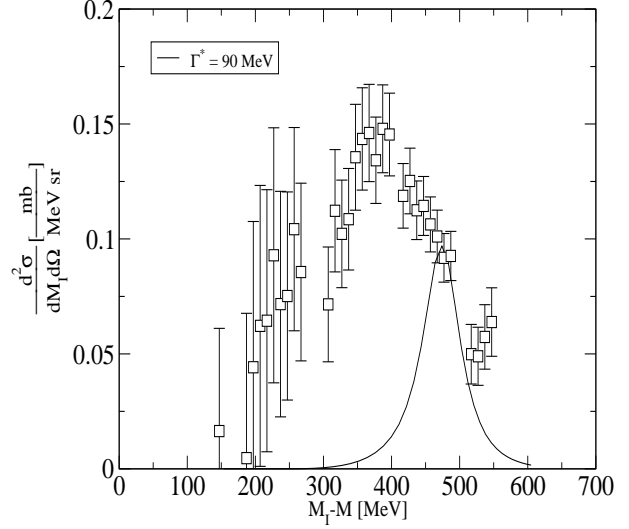


Fig. 4. Quark model result for the RET process contributing to the $p(d, d')$ reaction. M_I is the invariant mass of the target system. Experimental data correspond to $T_d = 2.3$ GeV and $\theta^L = 1.1$ deg. They were obtained in Ref. [16] by means of a theoretical subtraction of the Δ contribution.

based potential has a non-trivial structure. Due to the presence of the antisymmetrizer we have that, for instance, a scalar coupling at quark level gives rise to a scalar, spin-spin, pseudoscalar and pseudovector couplings [17]. The extraction of the scalar part can be done once the unprojected potential for different (ST) channels has been evaluated in the form:

$$V_{NN \rightarrow NN^*}^{(S,T)}(\mathbf{q}) = \frac{4\pi}{\mathcal{N}^{ST}} \sum_{JM_J}^{J_{MAX}} \sum_{LM_L} \sum_{M_S} C_{JM_J}^{LSM_L M_S} Y_{LM_L}(\hat{q}) \int_0^\infty r^2 dr j_L(qr) \hat{V}_{NN \rightarrow NN^*}^{L,S;JT}(r), \quad (12)$$

where we are adding up the partial waves up to a certain J_{MAX} . \mathcal{N}^{ST} is the unprojected norm of the $NN^*(1440)$ system and $\hat{V}^{L,S;JT}$ is the projected potential multiplied by the norm of the corresponding partial wave.

Then we write down the most general form for the interaction:

$$V_{NN \rightarrow NN^*}^{(S,T)} = V_0 + V_1 \boldsymbol{\sigma}_1 \cdot \boldsymbol{\sigma}_2 + V_2 \boldsymbol{\tau}_1 \cdot \boldsymbol{\tau}_2 + V_3 \boldsymbol{\sigma}_1 \cdot \boldsymbol{\sigma}_2 \boldsymbol{\tau}_1 \cdot \boldsymbol{\tau}_2. \quad (13)$$

where V_i are functions of the interbaryon momentum, $\boldsymbol{\sigma}_i$ and $\boldsymbol{\tau}_i$ are spin and isospin matrices of the baryons. V_0 is the scalar part of the total potential which is the only part that can be included in our process of $N^*(1440)$ excitation in $p(d, d')$ reactions.

Finally, if we consider different (ST) channels, we obtain the following system of equations,

$$V_{NN \rightarrow NN^*}^{(0,0)} = V_0 - 3V_1 - 3V_2 + 9V_3$$

$$\begin{aligned}
 V_{NN \rightarrow NN^*}^{(1,0)} &= V_0 + V_1 - 3V_2 - 3V_3 \\
 V_{NN \rightarrow NN^*}^{(0,1)} &= V_0 - 3V_1 + V_2 - 3V_3 \\
 V_{NN \rightarrow NN^*}^{(1,1)} &= V_0 + V_1 + V_2 + V_3,
 \end{aligned} \tag{14}$$

and solving for the scalar part,

$$\begin{aligned}
 V_0 &= \frac{1}{16} \left[V_{NN \rightarrow NN^*}^{(0,0)} + 3V_{NN \rightarrow NN^*}^{(0,1)} + \right. \\
 &\quad \left. 3V_{NN \rightarrow NN^*}^{(1,0)} + 9V_{NN \rightarrow NN^*}^{(1,1)} \right].
 \end{aligned} \tag{15}$$

We focus our attention on the target Roper excitation process. To compare to data it is necessary to subtract the Δ contribution and the interference term from the experimental points. The parameters of the Δ excitation on the projectile used in the phenomenological model were settled in the (α, α') reaction. We assume this process to be correctly described. Therefore we consider the data where the Δ contribution has already been subtracted [16] as our experimental data.

In Fig. 4 we show the result obtained using the quark-model derived $NN \rightarrow NN^*(1440)$ potential and its comparison to data. As can be seen, the predicted cross section is smaller than the model-dependent experimental data. If we choose a small value for the width of the $N^*(1440)$, the results come closer to the experimental data. Let us notice that the bigger disagreement with the extracted data corresponds to the region where the error bars are larger, in other words, to the region where the uncertainties related to the theoretical method used to subtract the Δ contribution and interference term are important. For the sake of clarity, let us note that the subtraction of the Δ contribution is proportional to the square of the $\pi N \Delta$

coupling constant. This coupling constant is different as used in baryonic processes, $f_{\pi N \Delta}^2/4\pi = 0.35$, as the one used in our quark model, $f_{\pi N \Delta}^2/4\pi = 0.22$ [18]. This value is crucial when trying to reproduce the 1S_0 NN phase shift through the tensor coupling to the 5D_0 $N\Delta$. Using the baryonic coupling one would obtain much bigger attraction than observed experimentally. As a consequence, the baryonic calculation of the Δ contribution could be underestimating the region above the peak overestimating in this way the $N^*(1440)$ contribution. The way to wipe out those uncertainties would be to calculate the Δ contribution together with the interference term making use of quark-model baryonic potentials.

It is also worth while to compare our results to the ones obtained from the baryonic calculation of the RET diagram [16]. To make more clear the comparison we plot the dependence of these results on the value chosen for the σ mass (within the allowed experimental interval), Fig. 5, and on the baryonic cut-off mass needed, Fig. 6. As can be seen the smaller m_σ the bigger the cross section and the smaller the cut-off the smaller the cross section. The significant dependence on the cut-off mass points out the need of having a good description of the scalar short-range part of the interaction. In our quark model framework this scalar piece is not uncertainly dependent on any free parameter but determined by quark antisymmetry plus the dynamics, the OPE and OGE giving most of the cross section, see Fig. 7. It is then clear that the results obtained with the quark-model derived interactions are qualitatively quite different to the ones reported using baryonic degrees of freedom. In fact, the baryonic form-factor could be hiding the effects of the quark substructure that we find in our quark-model treatment through the con-

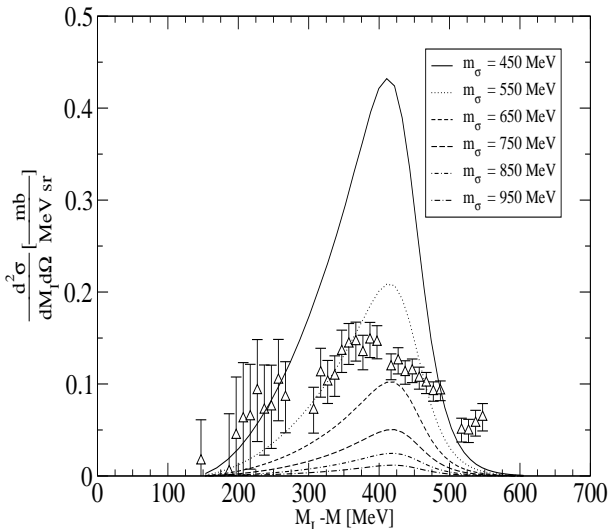


Fig. 5. Dependence of the $p(d, d')$ cross section calculated in Ref. [16] on the mass of the σ meson. M_T is the invariant mass of the target system. Experimental data correspond to $T_d = 2.3$ GeV and $\theta^L = 1.1$ deg. They were obtained in Ref. [16] by means of a theoretical subtraction of the Δ contribution.

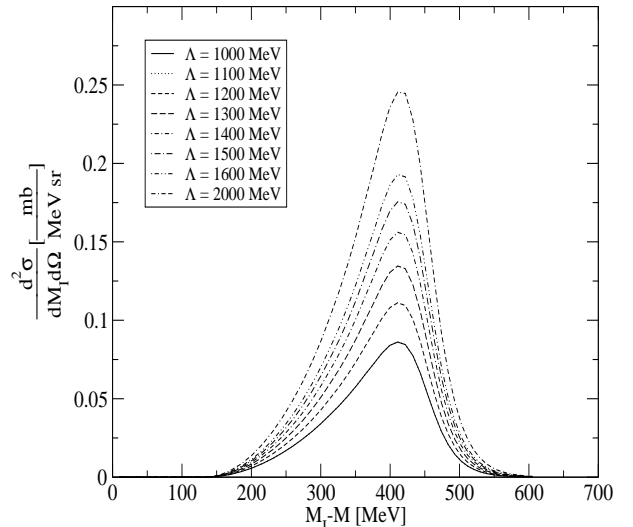


Fig. 6. Dependence of the $p(d, d')$ cross section calculated in Ref. [16] on the baryonic cut-off mass. M_T is the invariant mass of the target system.

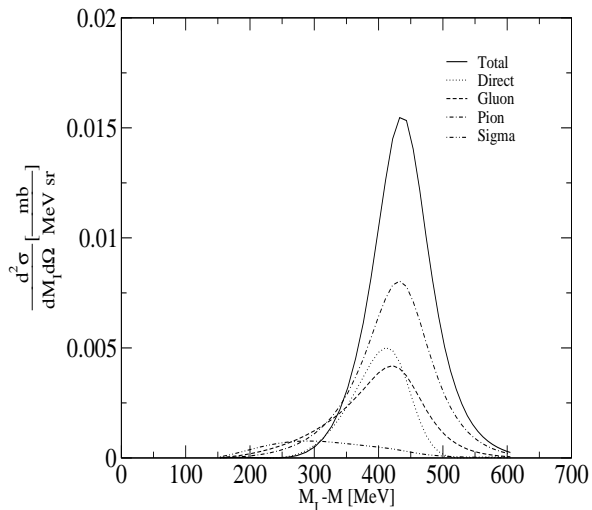


Fig. 7. Detailed contributions to the $p(d, d')$ cross section coming from the different interactions at the quark level, neglecting the interference terms. We denote by direct the result obtained neglecting quark-exchange diagrams. M_T is the invariant mass of the target system.

tributions to the scalar channel from every term in the quark-quark Hamiltonian.

4 Summary

We have carried out a test of a quark-model based $NN \rightarrow NN^*(1440)$ potential derived from an universal qq interaction. The consideration of the long-range tail of the potential as compared to the baryonic parametrization allows the extraction of the $\pi NN^*(1440)$ and $\sigma NN^*(1440)$ coupling constants. On the other hand the consideration of the physical mechanisms involved in the reactions $p(\alpha, \alpha')$ and $p(d, d')$, in particular the RET, allows to test the scalar short-range part of the interaction. The results we get are quite encouraging in spite of the lack of a full quark model calculation. To pursue this could open a new way to search for effects of the microscopic structure in the mentioned processes.

5 Acknowledgments

The authors thank Dr. S. Hirenzaki for useful correspondence concerning the calculation of Ref. [16]. This work has been partially funded by Ministerio de Ciencia y Tecnología under Contract No. BFM2001-3563, by Junta de Castilla y León under Contract No. SA-109/01, and by EC-RTN (Network ESOP) under Contracts No. HPRN-CT-2000-00130 and HPRN-CT-2002-00311.

References

1. K. Hagiwara *et al*, Phys. Rev. D **66** (2002) 010001.
2. M.T. Peña, D.O. Riska, and A. Stadler, Phys. Rev. C **60** (1999) 045201.
3. S. Hirenzaki *et al*, Phys. Lett. B **378** (1996) 29; Phys. Rev. C **53** (1996) 277.
4. L. Alvarez-Ruso, Phys. Lett. B **452** (1999) 207.
5. B.A. Li, C.M. Ko, and G.Q. Li, Phys. Rev. C **50** (1994) 2675.
6. S. Huber and J. Aichelin, Nucl. Phys. A **573** (1994) 587.
7. H. Garcilazo and E. Moya de Guerra, Nucl. Phys. A **562** (1993) 521.
8. A. Valcarce, F. Fernández, H. Garcilazo, M.T. Peña, and P.U. Sauer, Phys. Rev. C **49** (1994) 1799.
9. B. Juliá-Díaz, A. Valcarce, P. González, and F. Fernández, Phys. Rev. C **66** (2002) 024005.
10. D.R. Entem, F. Fernández, and A. Valcarce, Phys. Rev. C **62** (2000) 034002.
11. K. Holinde, Nucl. Phys. A **415** (1984) 477.
12. D.O. Riska and G.E. Brown, Nucl. Phys. A **679** (2001) 577.
13. S. Hirenzaki, P. Fernández de Cordoba, and E. Oset, Phys. Rev. C **53** (1996) 277.
14. H.P. Morsch *et al*, Phys. Rev. Lett. **69** (1992) 1336.
15. P. Fernández de Cordoba *et al*, Nucl. Phys. A **586** (1995) 586.
16. S. Hirenzaki, E. Oset, C. Djalali, and M. Morlet, Phys. Rev. C **61** (2000) 044605.
17. T.E.O. Ericson and W. Weise, *Pions and Nuclei* (Oxford, Clarendon, 1988).
18. A. Valcarce, A. Faessler, and F. Fernández, Phys. Lett. B **345** (1995) 367.

